Improved Hydrometeorological Forecasting through Physically-based Distributed Models

Semiannual report: 10/30/2008

Enrique R. Vivoni, Lead Investigator
Department of Earth and Environmental Science
New Mexico Institute of Mining and Technology (NMT)
801 Leroy Place, MSEC 244Socorro, NM 87801
Tel. (505) 835-5611, Fax (505) 835-6436
Email. vivoni@nmt.edu

David J. Gochis, Co-Investigator
Research Applications Program
National Center for Atmospheric Research (NCAR)
3450 Mitchell Lane, Boulder, CO 80307
Tel. (303) 497-2809, Fax. (303) 497-8401
Email: gochis@rap.ucar.edu

Table of Contents

List of Figures

List of Tables

Abstract

This report summarizes the advances relating the regional collection of data and the hydrologic modeling process in experimental watersheds within the Colorado Front Range (CFR). Eleven subbasins, belonging to the Big Thompson, Saint Vrain, Boulder and Coal Creek, and their most relevant data sets, have been collected during this project period. These basins have been selected through a multiple step analysis based on available data and hydrological properties. They span a large range of contributing areas and are characterized by a minimal influence of management operations, thus ensuring natural hydrologic response. Digital elevation models, basin boundaries, stream networks, soil and vegetation maps, and hydrometeorological observations have been collected to provide input and verification data for the hydrologic modeling efforts in the project.

Quantitative precipitation forecasts (QPFS) have been developed for the hydrological modeling domain using three different approaches; two from numerical weather prediction (NWP) models and one from a radar nowcasting (extrapolation) algorithm. The nowcasting algorithm used is the NCAR Thunderstorm IdenTification Analysis and trackiNg (TITAN) system which is capable of producing skillful QPFs out to about one hour depending on storm conditions. The NWP QPF products are derived from the operational North American Model (NAM) executed by the National Center for Environmental Prediction (NCEP) and the Advanced Weather Research and Forecasting (WRF) Model. Each QPF product is generated on a 1 km x 1 km Cartesian grid over the CFR region and the details of each are described below.

We present a set of preliminary simulations with the TIN-based Real-time Integrated Basin Simulator (tRIBS) model for Fish Creek watershed, using NEXRAD-MPE precipitation estimates that have been processed for the CFR. Our reported initial simulations span the period July 1st to 30th, 2004. Simulated streamflows for this basin are strongly dependent on the initial conditions. Hence, different groundwater table initialization strategies were tested, obtaining differences between observed and simulated discharges. Further steps will focus on systematic calibration strategies in order to address the two main science questions of the planned forecasting experiments.

1. Introduction and Literature Review

Scientific questions addressed in this project focus on the lead-time dependence and catchment scale variability of the flood forecast skill in the CFR. Several studies have discussed the importance of these questions (Browning and Collier, 1989; Collier and Krzysztofowicz, 2000; Lin et al, 2005; Benoit et al, 2000 and Vivoni et al, 2006a,b). We argue that improved flood forecast skill can only be adequately addressed through a physically-based hydrometeorological modeling process. Consequently, a modeling approach that minimizes the error sources during the data collection and model parameterization can maximize the similarity between observations and simulations. Special care should be taken with the hydrometeorological information collection and processing. Processing

and model setup deserve exceptional attention, in particular, initial and boundary conditions, and model parameterization. Some authors have already addressed the issue of model parameterization, obtaining field values consistent with laboratory tests (Rutter et al 1975, Ivanov et al 2004; Brutsaert 2005; Rawls et al 1983; Ogden 1997; Mahmood and Vivoni, 2008).

This semiannual report includes four main sections, each of them related to the completion of the first year goals scheduled in the project timeline. Our efforts were focused on data collection, model set up and design of a forecasting experiment. In section 2, there is detailed information concerning the stage of the hydrologic and meteorological data collection: topography, soils and vegetation as well as radar precipitation products and streamflow-discharge observations, for eleven watersheds in CFR. Section 3 describes the development of the three different QPF products occurring during the year 1. Finally, the tRIBS model was setup for the Fish Creek basin and initial modeling experiments were conducted under several initial conditions. Results and discussion are compiled in section 4. Some conclusions and future work are summarized in section 5.

2. Hydrometeorological Data Collection

Improved flood forecasting skill will be sought via numerical experiments at Big Thompson, Saint Vrain, Boulder and Coal Creek watersheds. Calibration and validation of the simulated response will be based on comparisons with the observed discharge data at each stream gauge station installed by USGS and the Division for Water Resources of the Colorado State. Once confidence has been established in the distributed model simulations, numerical experiments will be conducted with a range of different quantitative precipitation estimates (QPEs) and quantitative precipitation forecasts (QPFs). This section discusses the hydrologic and meteorological data collection and processing.

2.1. Topography, Soils and Vegetation Maps

The selected watersheds are located in the counties of Larimer, Boulder, Gilpin and Jefferson, Colorado. All of them are sub-basins of the Big Thompson, Saint Vrain, Boulder and Coal Creeks. A 30-m pixel size digital elevation model was downloaded from USGS. This DEM was corrected for pits and barriers in the streamflow network and finally converted to a Triangulated Irregular Network (TIN, see section 4.2). Figure 1 illustrates the topographic distribution and watershed divides for the CFR study basins. Table 1 presents the drainage area of each sub-basin and the corresponding regional or major basin. The basin areas range between 35 to 359 km^2. Watersheds were selected that did not have significant hydraulic infrastructure. However, several basins have the presence of snow in the winter and hence, a snowmelt signal is expected in the streamflow time series. Topographic variations are due to the nature of the watersheds on the east flank of the CFR. Maximum elevation for the system of basins is 3900 m, whereas the minimum is approximately 1600 m. Landscape variations are remarkable with a generalized east-facing aspect. The Horton order ranges from 2 for small basins to 4 for larger reaches. Table 2 summarizes some topographic and morphometric characteristics of the basins.
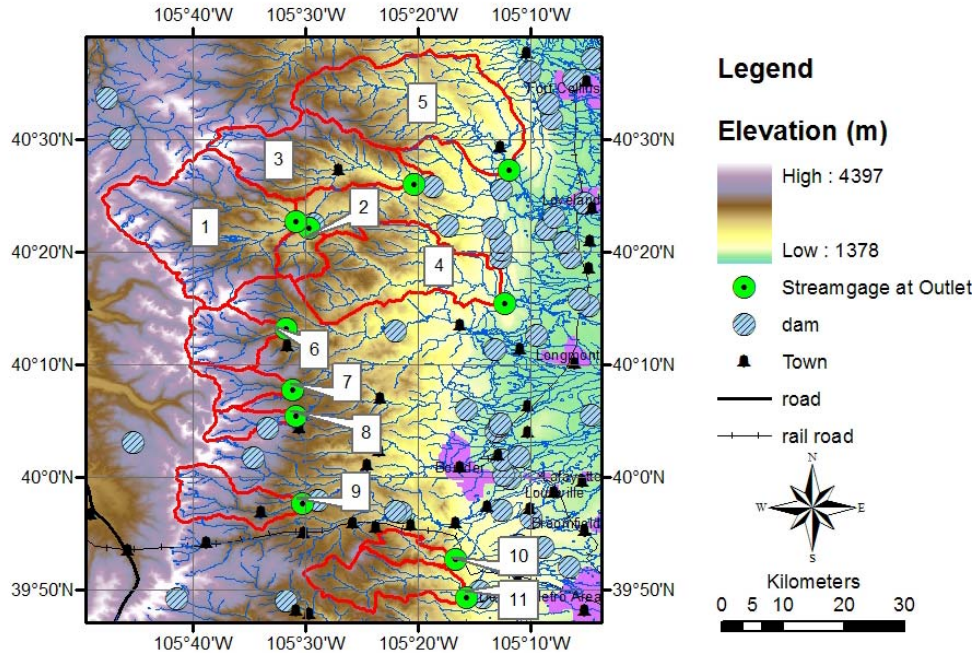
Figure 1. Watershed divides, streamlines and digital elevation model of the CFR study area

Table 1. Characteristics of the study watersheds and USGS gauging stations.

N°	Subbasin	Area (km^2)	Outlet	Major Basin
1	Big Thompson River at Estes Park	359.49	BTABESCO	Big Thompson River
2	Fish Creek Near Estes Park	40.84	FISHESCO	Big Thompson River
3	North Fork Big Thompson River at Drake	220.70	BTFDRCO	Big Thompson River
4	Little Thompson River Near Berthoud	258.50	LTCANYCO	Big Thompson River
5	Buckhorn Creek near Masonville	350.50	BUCRMVCO	Big Thompson River
6	North Saint Vrain Creek Near Allens Park	88.48	STALENCO	Saint Vrain Creek
7	Middle Saint Vrain Creek Near Peaceful Va	49.90	MIDSTECO	Saint Vrain Creek
8	South Saint Vrain Creek Near Ward	35.10	SSVWARCO	Saint Vrain Creek
9	Middle Boulder Creek at Nederland	95.47	BOCMIDCO	Boulder Creek
10	Coal Creek Near Planview	37.16	COCPRECO	Boulder Creek
11	Ralston Creek Ab. Reservoir Near Golden	117.30	RALCRKCO	Clear Creek

A soil type distribution in Figure 2 was constructed from several county maps from the Soil Survey Geographic (SSURGO) database, originally at a scale of 1:24000. This database is manipulated with an ACCESS tool from the U.S Natural Resources Conservation Service which assigns a dominant soil textural class to every polygon. Those categories have modifiers that give details for the fraction of other textures. Therefore, the twelve common soil textural classes plus eight additional types, accounting for stones, fragments, water, and peat, were assigned with parameter values in the model using literature values and studies performed in similar regions (Ivanov et al, 2004; Rawls et al 1983; Ogden 1997; Mahmood and Vivoni, 2008). Missing polygons in SSURGO were filled in with STATSGO information at scale 1:250,000. Tables 3 and 4 show a detailed view to the model parameters and values. Figure 3 illustrates a histogram of the soils coverage for the CFR region; decomposed plant material, sandy loam, loam and unweathered rock are the dominant classes.

Table 2. Some morphometric characteristics of the study watersheds.

| N°	Subbasin	Area (km^2)	Elevations range (m)	Mean elevation (m)	Elevation standard deviation (m)	Horton Order
1	BTABESCO	359.49	[2289, 4338]	3253	574	4
2	FISHESCO	40.84	[2294, 3454]	2854	329	2
3	BTFDRCO	220.70	[1944,4080]	2984	640	3
4	LTCANYCO	258.50	[1595, 3434]	2505	526	4
5	BUCRMVCO	350.50	[1585, 3242]	2420	483	4
6	STALENCO	88.48	[2526,4344]	3396	504	3
7	MIDSTECO	49.90	[2635, 4029]	3318	395	2
8	SSVWARCO	35.10	[2860, 4088]	3461	348	2
9	BOCMIDCO	95.47	[1993, 3204]	2582	342	3
10	COCPRECO	37.16	[2497, 3987]	3235	427	2
11	RALCRKCO	117.30	[1847, 3190]	2510	383	2
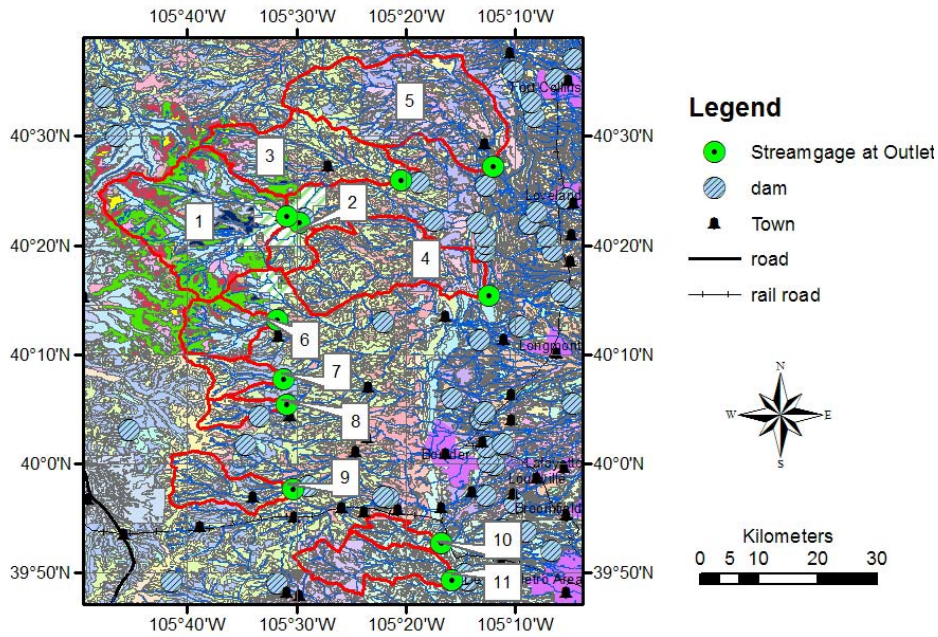
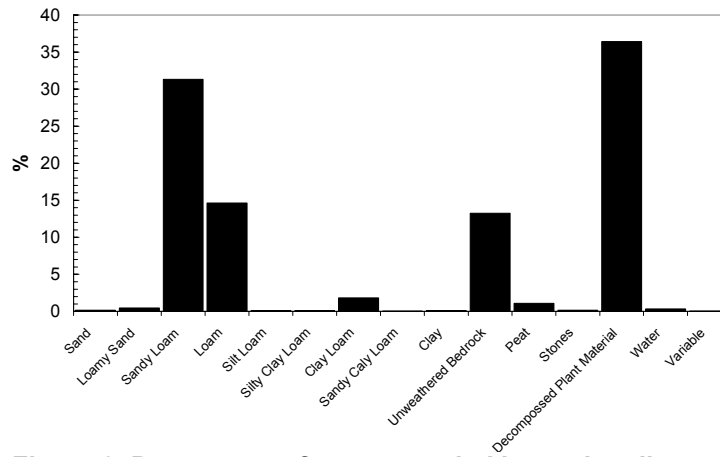**Figure 2. Soils map for the CRF study region with labeled study basins.**

Figure 3. Percentage of area occupied by each soil type.

4

Table 3. Soil parameter descriptions.

Description	Parameter	Units
Saturated Hydraulic Conductivity	K_s	[mm/h]
Soil Moisture at Saturation	θ_s	[ ]
Residual Soil Moisture	θ_r	[ ]
Pore Distribution Index	m	[ ]
Air Entry Bubbling Pressure	ψ_b	[mm] (negative)
Decay Parameter	f	[mm^{-1}]
Saturated Anisotropy Ratio	A_s	[ ]
Unsaturated Anisotropy Ratio	A_u	[ ]
Porosity	n	[ ]
Volumetric Heat Conductivity	k_s	[J/msK]
Soil Heat Capacity	C_s	[J/m^{3}K]

Table 4. Soil parameterization for tRIBS model application.

SSURGO classification	K_s	θ_s	θ_r	m	Ψ_b	f	A_s	A_u	n	k_s	C_s
Stones	3600	0.400	0.05	0.600	-100	0.007	25	125	0.400	1	10^6
Fragments	1800	0.400	0.05	0.600	-100	0.007	25	125	0.400	1	10^6
Weathered Bedrock	200	0.400	0.05	0.600	-100	0.007	25	125	0.400	1	10^6
Sand	117.8	0.417	0.020	0.592	-73	0.007	65	140	0.437	1	10^6
Loamy sand	29.9	0.401	0.036	0.374	-87	0.007	65	140	0.437	1	10^6
Sandy Loam	10.9	0.412	0.041	0.378	-146.6	0.00520	65	140	0.453	1	10^6
Loam	3.4	0.434	0.027	0.252	-111.0	0.00625	25	125	0.463	1	10^6
Sandy Clay Loam	1.5	0.330	0.068	0.242	-120.0	0.00670	25	125	0.398	1	10^6
Unweathered bedrock	19.9	0.085	0.015	0.165	-373.3	0.00157	25	125	0.150	1	10^6
Variable	2.0	0.400	0.050	0.252	-208	0.0070	25	125	0.400	1	10^6
Silt	6.5	0.486	0.015	0.234	-208	0.0070	65	140	0.501	1	10^6
Silt Loam	6.5	0.486	0.015	0.234	-208	0.0065	65	140	0.501	1	10^6
Silt Clay Loam	1.0	0.432	0.039	0.234	-240	0.0068	50	140	0.471	1	10^6
Clay Loam	1.0	0.309	0.155	0.240	-259	0.0070	50	140	0.464	1	10^6
Sandy Clay	0.6	0.321	0.109	0.242	-300	0.0070	50	140	0.430	1	10^6
Silt Clay	0.5	0.423	0.056	0.242	-350	0.0070	50	140	0.479	1	10^6
Decomposed plant material	29.9	0.401	0.036	0.374	-87	0.0070	65	140	0.437	1	10^6
Peat	29.9	0.401	0.036	0.374	-87	0.0070	65	140	0.437	1	10^6
Clay	0.3	0.385	0.090	0.150	-370	0.0070	50	140	0.475	1	10^6
Water	0.3	0.385	0.090	0.150	-370	0.0070	50	140	0.475	1	10^6

We collected 30 m pixel resolution vegetation maps from the USGS National Land Cover Data (NLCD), versions of 1992 and 2001. Figure 4 depicts distributed information of vegetation coverage types. An original set of 21 classes were reclassified into 8 dominant groups whose percentage of presence in the area is quantified in Figure 5. Forests, grasses and shrublands are the dominant vegetation over the region. Vegetation parameters have been published by Rutter et al (1975), Ivanov et al (2004) and Brutsaert (2005), among others. Some of those parameters will be modified as part of the calibration process and consistent values will be accomplished according to the hydrologic response. Table 5 contains a description of parameters and units, assigned to each soil type class in this experiment. A set of values used in the model parameterization is presented in Table 6.
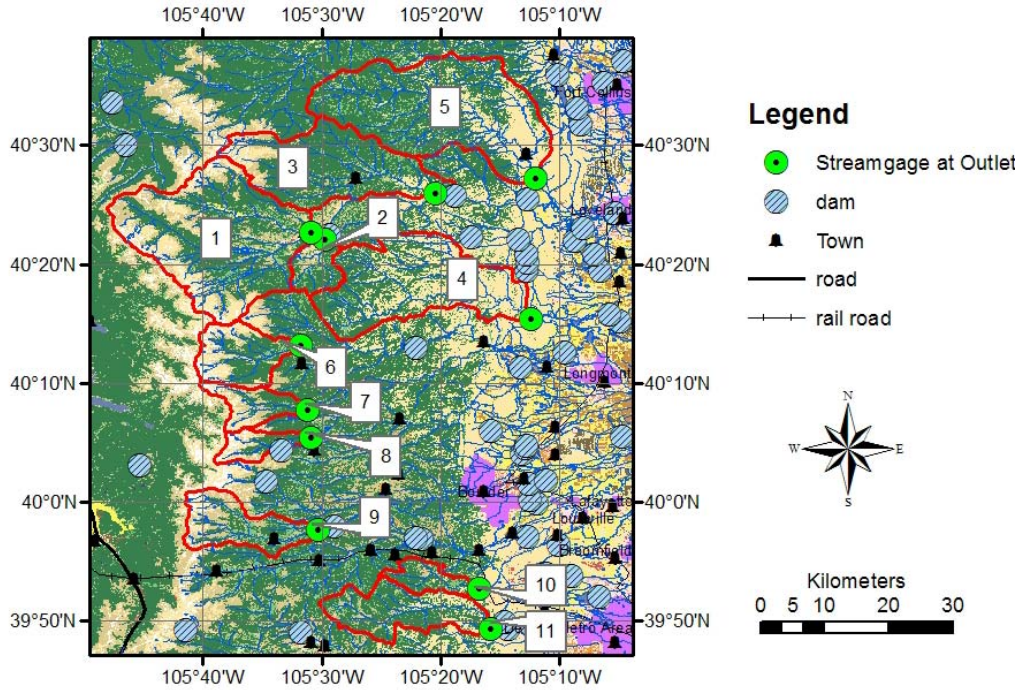
Figure 4. Vegetation map for the CRF.
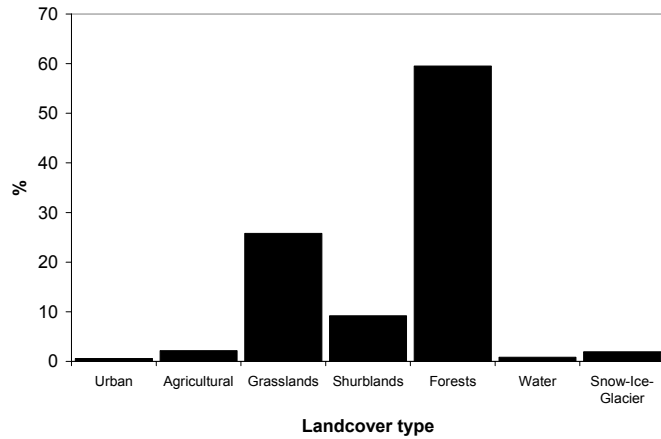
Figure 5. Percentage of area occupied by different vegetation types.

Table 5. Vegetation parameter description.

Description	Parameter	Units
Canopy Storage-Storage	a	[mm]
Interception Coefficient-Storage	b1	[ ]
Free Throughfall Coefficient- Rutter	P	[ ]
Canopy Field Capacity – Rutter	S	[mm]
Drainage Coefficient – Rutter	K	[mm/h]
Drainage Exponential Parameter - Rutter	b2	$[mm^{-1}]$
Albedo	Al	[ ]
Vegetation Height	h	[m]
Optical Transmission Coefficient	Kt	[ ]
Canopy-average Stomatal Resistance	Rs	[s/m]
Vegetation Fraction	V	[ ]
Canopy Leaf Area Index	LAI	[ ]

Table 6. Vegetation parameterization for tRIBS model application.

| Class/Par	a	b1	P	S	K	b2	Al	h	Kt	Rs	v	LAI
Urban	0.0	0.2	1.00	1.0	0.01	3.7	0.20	7.0	1.00	0.0	0.95	1.0
Agricultural	0.5	0.2	0.70	0.8	0.10	3.6	0.20	0.4	0.65	75.0	0.65	4.0
Grassland	0.5	0.2	0.85	0.8	0.10	4.2	0.15	0.2	0.70	50.0	0.50	4.0
Shrubland	0.5	0.2	0.70	1.5	0.20	3.9	0.16	0.8	0.55	100	0.50	5.0
Forests	1.1	0.2	0.48	2.4	0.12	3.7	0.12	10	0.45	150	0.80	6.0
Wetlands	0.0	0.0	1.00	1.0	0.01	3.7	0.04	0.01	1.00	0.0	0.95	0.0
Water	0.0	0.0	1.00	1.0	0.01	3.7	0.04	0.01	1.00	0.0	0.95	0.0
Ice-snow	0.0	0.0	1.00	1.0	0.01	3.7	0.90	0.05	1.00	0.0	0.95	0.0

2.2. Hydrometeorological Observations

2.2.1. NEXRAD MPE (QPE)

The Multisensor Precipitation Estimator (MPE) product was downloaded from the operational NOAA data archives for the MRBFC region and clipped to the CFR for use in the project. The MPE estimate has a temporal resolution of 1 hour and pixel size of 4 km. One-hour matrices were downloaded and processed for input to the hydrological models for the period January 1, 2003 to September 30, 2005 (latest date of available data). Preliminary analysis of rainfall allows concluding that the spatiotemporal variability of the precipitation is significant. Convective storms account for a great part of the maximum values recorded in the time series over this mountain region, as can be seen in Figures 6(a) and (b), where the hourly rain rates of one representative storm for July 16, 2004 at (a) 15h and (b) 17h have been estimated by the radar algorithms of the NEXRAD system over the CFR study area.
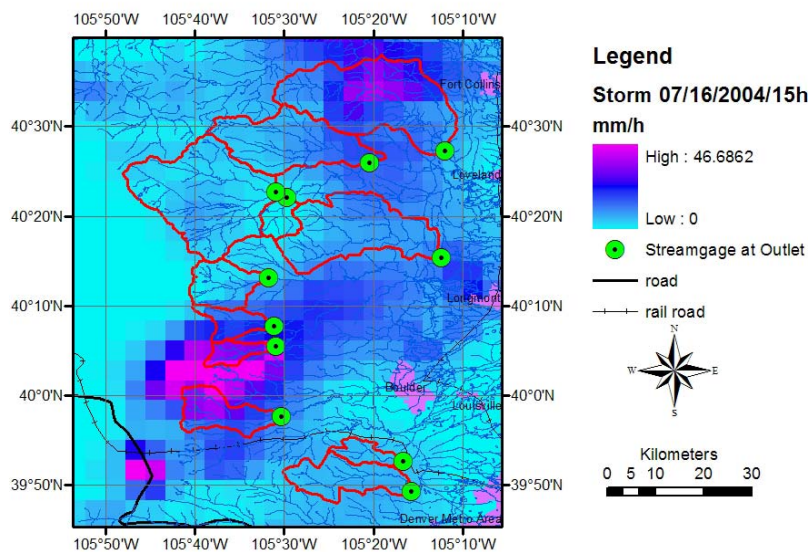
(a)
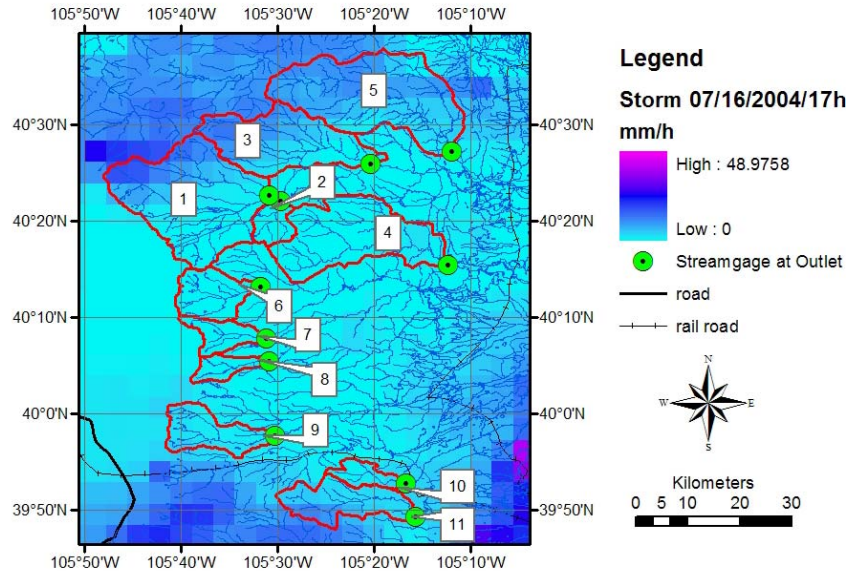
(b)

Figure 6. NEXRAD-MPE precipitation fields for July 16, 2004, at (a) 15 LST and (b) 17 LST over CFR basins.

To complement the MPE availability, we collected NEXRAD-Level II data. This precipitation product has a higher temporal resolution (5 min) of precipitation rates (mm/h) and a finer pixel size, 1 km. However, multiple gaps in the data set, spanning minutes to hours during storm events, will constrain the potential simulations to shorter periods of time or precipitation events of interest. We plan to compare the hydrological response to both precipitation products after we have performed model calibration based on the MPE product.

2.2.2. Observed Discharges

We collected streamflow observations from May 1st through September 30th of each year from 2003 to 2006 at 15 min temporal resolution. These were obtained from the Water Resources Division Office of Colorado. Streamflow time series show gaps or missing data, though these do not exceed 1% of the total record in all stations, with the exception of LTCANYCO with gaps of ~6%. The 15-minute data gaps were filled in using interpolation or the daily average values. Figure 7 illustrates five time series for the period July through September 2004. NEXRAD mean areal rainfall has been added on the top axis in order to correlate the actual discharges to estimated areal NEXRAD precipitation. At the beginning of July, the higher elevation basins seem to have snow signal in the streamflows. Discharges are in proportion to the basin area. Despite that they are relatively close to each other, the initial wetness conditions and the spatial variability of rainfall make the observed discharges different among the five watersheds. The largest discharges occur between July 15 to 30th, except in the Buckhorn Creek whose peak discharges occur in August 15th through 30th.
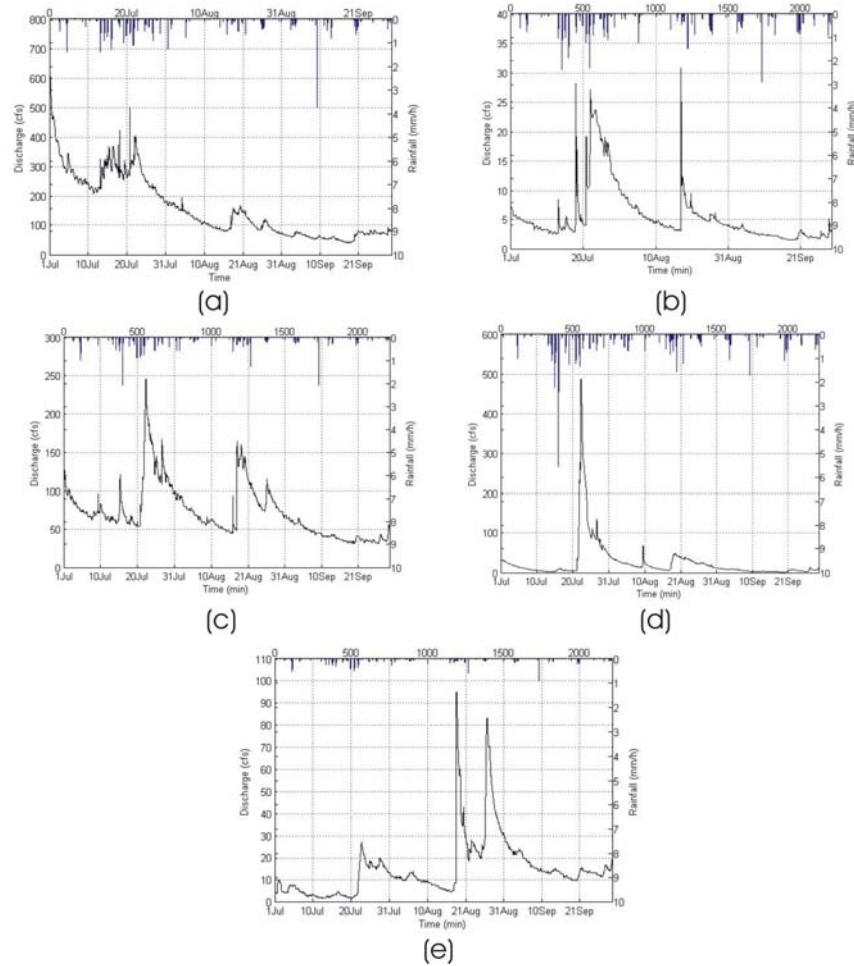
Figure 7. NEXRAD-MPE QPE and observed discharges for: (a) Big Thompson at Estes Park, (b) Fish Creek Near Estes Park, (c) North Fork at Drake, (d) Little Thompson near Berthoud and (e) Buckhorn Creek near Masonville.

2.2.3. Meteorological Observations

Time series of 40 meteorological stations in the area have been collected from different data sources. Almost all of them have precipitation, snow water equivalent (SWE) and temperature values and a few have wind speed and cloud cover. Some of the records needed to be filled in to remove gaps. Others are only available for the year 2007, but help as complementary climate information. Table 7 and Figure 8 summarize the main features of weather station data. The presence of such distributed configuration of weather stations ensures a consistent meteorological input to the hydrologic model. Satellite-based products and reanalysis data will help complementing meteorological time series.

Table 7. Available weather stations in the CFR.

| Nro	LAT (Deg)	LON (Deg)	ELEV (m)	START	TR	NRCSID	SITENAME
1	40.31	-105.64	9500	1/20/2000 0:00	today	BLKC2	Bear Lake
2	40.2	-105.567	8600	1/20/2000 0:00	today	COPC2	Copeland Lake
3	40.3058	-105.538	8920	11/17/2004 0:00	today	CO045	Lily Lake
4	40.43	-105.73	10700	1/20/2000 0:00	today	WPRC2	Willow Park
5	40.1803	-105.478	8241	3/10/2004 0:00	today	AR365	KM6GE Allenspark
6	40.221	-105.369	6500	5/16/2002 0:00	today	BTRC2	Button Rock
7	40.4333	-105.338	6170	3/13/2007 0:00	today	DKEC2	North Fork Big Thompson
8	40.3833	-105.483	7700	1/1/2005 0:00	today	CW3065	CW3065 Estes Park
9	40.3667	-105.55	7820	4/3/2001 0:00	today	ESPC2	Estes Park
10	40.6006	-105.171	0	3/23/2007 0:00	today	HR5C2	Horsetooth reservoir
11	40.3508	-105.171	5320	11/16/2005 0:00	today	C4671	CW4671 Loveland
12	40.5708	-105.227	6160	6/11/2004 0:00	today	RSOC2	Redstone
13	40.36083	-105.449	8573	6/25/2008 0:00	today	D0774	DW0774 Estes Park
14	39.81633	-105.183	5580	5/23/2007 0:00	today	C8064	CW8064 Westwood Links
15	39.8656	-105.24	6192	9/26/2005 0:00	today	CO109	N-93 - Jct. 93 & 72 (36)
16	39.87	-105.297	8050	5/16/2002 0:00	today	BMTC2	Blue_Mountain
17	39.9136	-105.247	6086	6/9/2004 0:00	today	NWTC	Rocky Flats Nat Wind Tech Ctr
18	39.9781	-105.276	6184	5/16/2002 0:00	today	NCARM	NCAR Table Mesa
19	39.8243	-105.48	9370	1/15/2006 0:00	today	C5066	CW5066 Gilpin Co.
20	40.0181	-105.361	6733	6/26/2001 0:00	today	BTAC2	SUGARLOAF
21	40.018	-105.404	7860	5/16/2002 0:00	today	SFSC2	Sugarloaf
22	40.0433	-105.278	5217	9/10/2003 0:00	today	AP115	AB0MY-2 Boulder
23	40.035	-105.243	5331	5/16/2002 0:00	today	NCARF	NCAR Foothills Lab
24	40.071	-105.193	5239	10/10/2007 0:00	today	C8872	CW8872 Gunbarrel
25	40.08294	-105.346	7349	9/8/2007 0:00	today	C8656	CW8656 Boulder
26	40.04	-105.54	9910	1/20/2000 0:00	today	NIWC2	NIWOT
27	40.03	-105.58	10300	1/20/2000 0:00	today	UVCC2	UNIVERSITY CAMP
28	40.04278	-105.592	10692	9/26/2005 0:00	today	ALBIO	Niwot Ridge Albion
29	40.05472	-105.589	11575	5/18/2002 0:00	today	SADDL	Niwot Ridge Saddle
30	40.08267	-105.497	9155	11/17/2004 0:00	today	CO044	Ward (35)
31	40.148	-105.39	7760	5/16/2002 0:00	today	CALC2	Cal-Wood_Ranch
32	40.18806	-105.501	8215	6/6/2001 0:00	today	ALKC2	ALLENSPARK 2SE
33	40.2	-105.6	9560	6/25/2003 0:00	today	WLBC2	WILD BASIN
34	39.94	-105.59	9700	1/20/2000 0:00	today	LELC2	LAKE ELDORA
35	39.8444	-105.517	9380	4/3/2001 0:00	today	PKLC2	PICKLE GULCH
36	39.92	-105.76	9680	1/21/2000 0:00	today	AROC2	ARROW
37	39.87933	-105.491	9301	1/30/2008 0:00	today	C9764	CW9764 Black Hawk
38	39.81133	-105.644	10000	3/5/2008 0:00	today	D0063	DW0063 Idaho Springs
39	39.7944	-105.763	12490	6/20/2007 0:00	today	K0CO	Berthoud Pass Heliport
40	39.8	-105.78	11300	1/20/2000 0:00	today	BTSC2	BERTHOUD SUMMIT

10
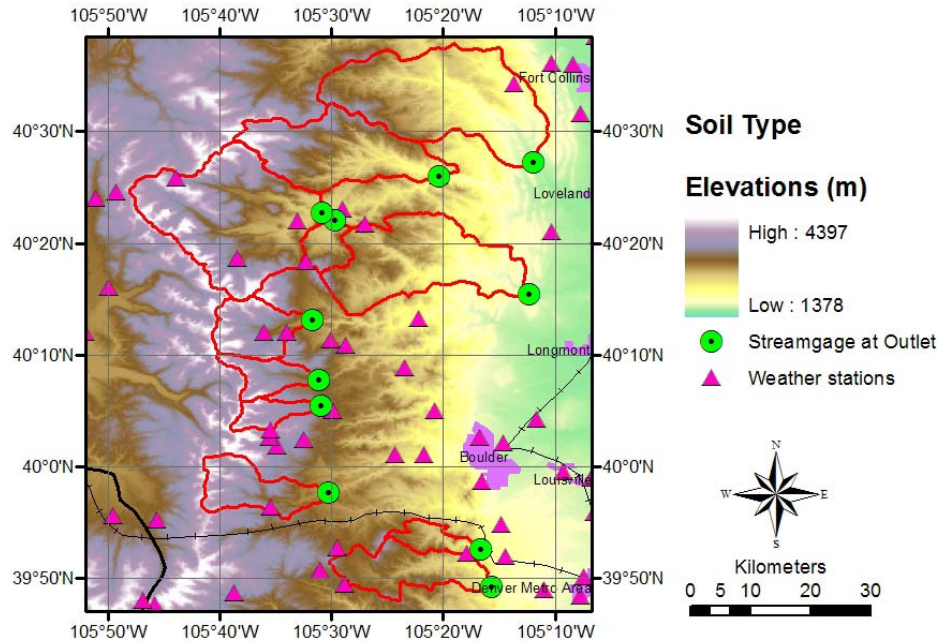
Figure 8. Spatial distribution of the weather stations in CFR.

3. Quantitative Precipitation Forecasts (QPFs)

To produce observed catchment responses to precipitation forcing, it is critical to generate QPFs that possess as nearly identical space-time covariance and intensity structures as possible to those that occurred. The generation of QPFs remains a grand challenge and yet unresolved issue in the atmospheric and hydrologic sciences. However, in this project, we employ two distinct, state of the art methodologies for generating QPFs on two distinct forecast lead times; very short term (0 – 60 min) and daily (6-36 hours). Additionally, as a reference we also employ the operational U.S. national forecast model (NAM) QPFs, though it is acknowledged that this product is likely to have large deficiencies in accurately forecasting flash flood producing rain events. Hence, three separate QPF products have been developed for use in this project, as described below.

Very short term QPFs are generated from Level II NEXRAD data using the NCAR TITAN algorithm (Dixon, 1994). In conjunction with additional NCAR radar processing algorithms, Level II reflectivity data is ingested in real-time and then subject to Cartesian projection, bright band filtering, de-cluttering, hail thresholding, and rain rate estimation. As described in Dixon (1993), the TITAN system identifies storm objects, or ellipses, based on time-series of radar reflectivity or rain rate imagery where a pre-specified threshold has been met. The storm propagation vector and ellipse growth and decay parameters diagnosed from the storm time-series are then extrapolated forward in time in a time-invariant way to generate an extrapolated QPF field out to 60 minutes. In the coming year, we will cast these extrapolation parameters in a probabilistic framework in order to generate ensembles of very short term QPF for use in flash flood prediction in the CFR region.

11

Initial selection of the reflectivity-rain-rate (Z-R) relation was Z=500R^1.6, derived through comparison with surface rain gauges and based upon a selection of warm season events from June and July of 2008. This specification of Z-R reflects a significant loss of precipitation due to subcloud evaporation that is common in warm season convective events in the CFR region. It is wholly acknowledged that Z-R relationships vary widely in time and in space and it is nearly impossible to define a single optimal Z-R relationship for any significant period of time. Nevertheless, Kelsch et al. (1988) in a survey of CFR convective storms also found a Z-R of Z=500R^1.3, so it is felt that use of our initial Z-R relationship is justified pending additional comparisons.

QPFs on the daily timescale were generated using two different NWP models, the NCAR Advanced Weather Research and Forecasting (WRF) model and the NCEP North American Model (NAM). Although both of these NWP models are variations of the same modeling architecture, for our purposes, the most significant differences are that the WRF model is executed on a 1 km, cloud system resolving grid where convective parameterization is not required and a modestly different suite of model physics parameterizations is used. Conversely, the NAM model operated by NCEP is executed on a 12 km grid and convection is parameterized. We generate one 36-hour, 1 km WRF forecast daily using initial conditions specified by the NOAA Forecast Systems laboratory Rapid Update Cycle (RUC) model and boundary forcing provided by the NCEP Global Forecast System (GFS) model. To facilitate use of the NAM model for flash flood prediction, we simply regrid the QPF values from the native 12 km grid to a 1 km grid without any posterior correction thus preserving the original structure of the forecasted rainfall.

Each product was generated in a real-time forecast demonstration project during the summer of 2008. Quantitative evaluation of their accuracy is currently underway and the results of this analysis will be presented at the upcoming annual meeting of the American Meteorological Society in January of 2009. Figure 9 illustrates the NEXRAD derived rainfall for the 1997 Fort Collins flash flood along with the hydrologic model domain in CFR.
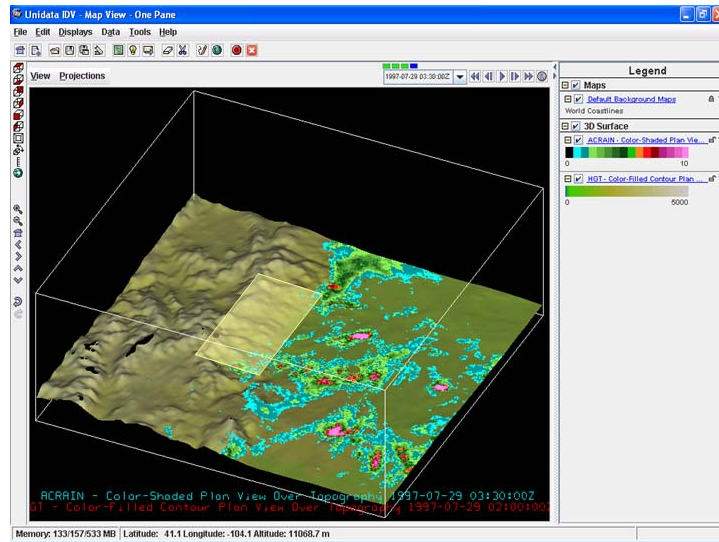
Figure 9. Full Front Range QPF domain and sample depiction of NEXRAD derived rainfall for the 1997 Fort Collins Flash Flood event. Inset box with transparent shading outlines the tRIBS modeling domain.

4. Hydrologic Simulations in an Experimental Watershed

The TIN-based Real-time Integrated Basin Simulator (tRIBS) distributed model captures spatial heterogeneities in catchment properties, resolves spatial-temporal variability in hydrometeorological forcing, and simulates fine-scale hydrologic fields and streamflow hydrographs at multiple, nested locations. In this project, we will evaluate the performance of the distributed model for several flood events of interest. We commenced our work by selecting a few events in July 2004, when discharge values were recorded by the USGS gauges and we had available MPE and NEXRAD-Level II data. As inputs to the distributed model, vegetation, soils and TIN domains were prepared to be ingested by the model. Complementarily, NEXRAD hourly precipitation and meteorological time series were used as climatic input. Since initial values of the groundwater field were unknown (due to the lack of field measurements), preliminary drainage and spin up experiments were performed in order to estimate appropriate values for the initialization condition.

4.1. Model Domain Representation

Fish Creek watershed was selected to carry out a preliminary set of model simulations using tRIBS. This simulation was performed for a period of 30 days (July 1 to 30, 2004) since this included a series of significant precipitation events during the summer season. For the preliminary simulations, we are not considering the potential effects of the spring snowmelt on the runoff production.

A Triangulated Irregular Network (TIN) of 14,782 nodes was constructed for the domain representation in the form of the associated Voronoi polygons. Figure 9 illustrates the DEM, TIN and Voronoi polygons generated for the preliminary simulation. Notice that the finest discretization is accomplished in the vicinity of the main channel, ensuring accurate spatial representation of runoff production. In this case, the grid reduction factor was chosen as d = 0.2, implying
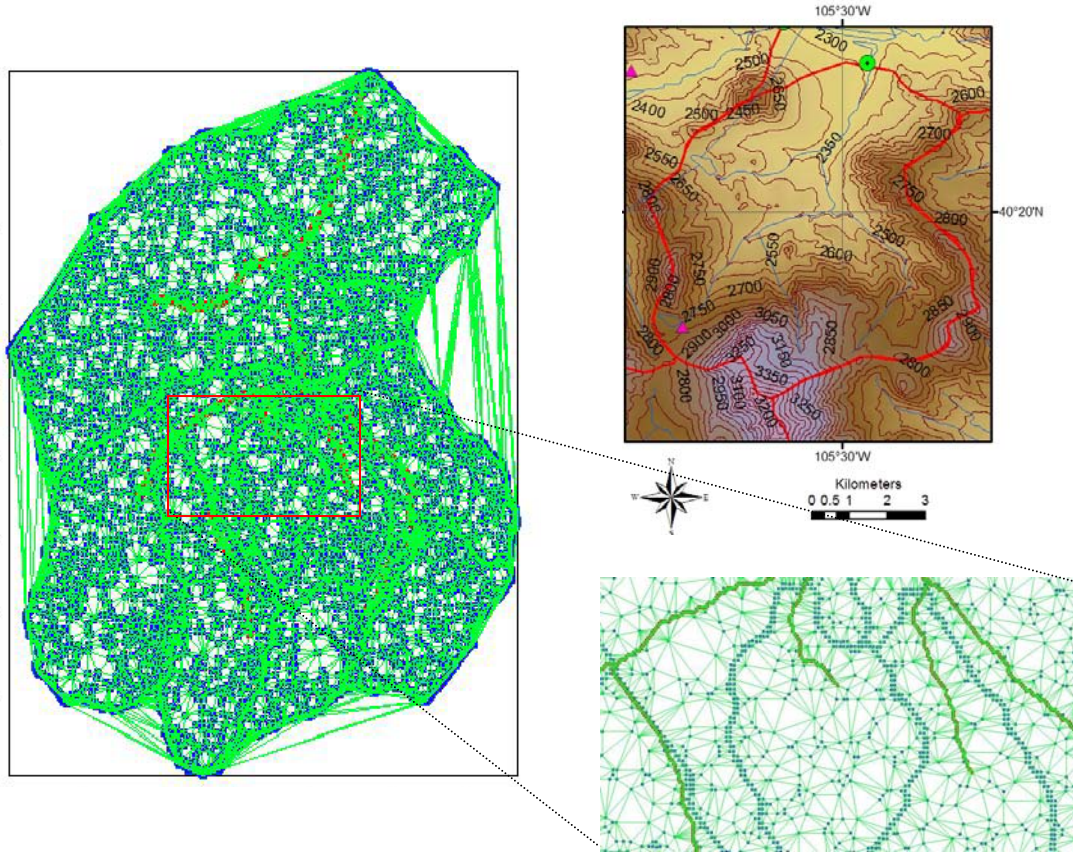
Figure 10. Topographic configuration and geometry of the Triangulated Irregular Network for the Fish Creek watershed.
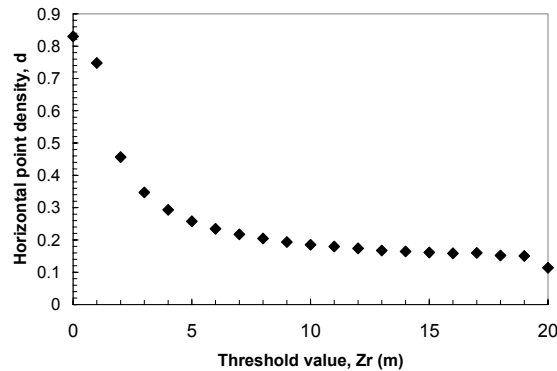

Figure 11. TIN aggregation properties. Horizontal point density, *d*, as a function of the allowed error tolerance z_r.

that only 20% of the original DEM nodes were retained. Figure 10 illustrates the behavior of the threshold value z_r with *d* for the Fish Creek basin. The relative small basin will lead to a fast hydrograph response to precipitation which may be accentuated by presence of high average antecedent soil moisture.

Vegetation distribution for Fish Creek is shown in Figure 11 (a), along with a false color Landsat image, taken on 06/23/2004 (b). Due to its mountainous setting, Fish Creek is dominated by forest vegetation along with contributions of

urban, agricultural land and shrubs, near Estes Park Town (north-west). Such configuration, with contrasting land uses, governs the distribution of interception and evapotranspiration parameters over the surface and vegetation canopy.

Same contrasting behavior is presented by the soils distribution, which is shown in Figure 12. The sharp boundary is the effect of the filling in process of SSURGO from STATSGO information. The two dominant soil types, sandy loam and decomposed plant material determine the distribution of the soil moisture through soil hydraulic and thermal properties. Decomposed plant material, classified with a relatively high hydraulic conductivity, combined with the forest dominance, will impose a condition of high infiltration and recharge rates in the south and south-eastern parts of Fish Creek basin.
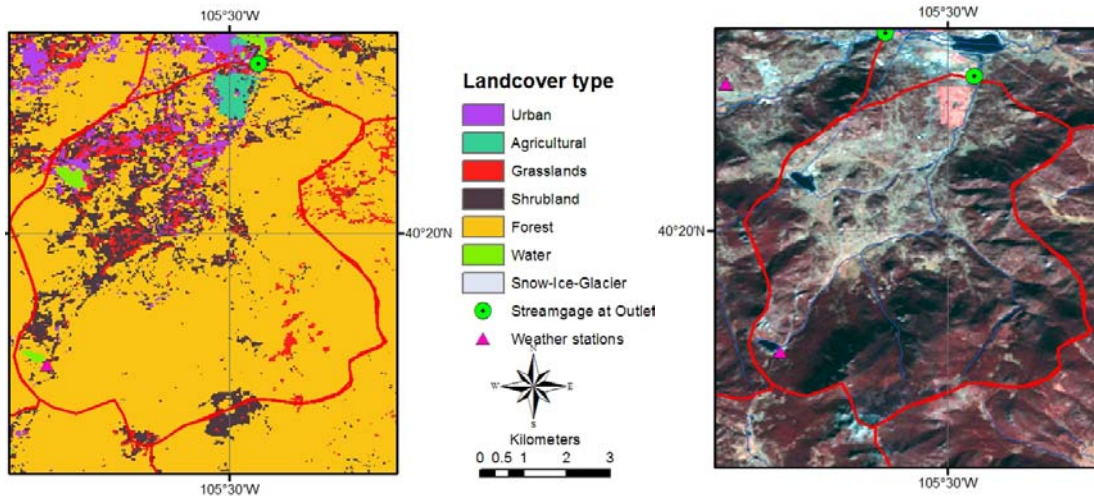

Figure 12. (a) Vegetation distribution in Fish Creek watershed from NLCD map. (b) 06/23/2004 false color Landsat 30-m image.
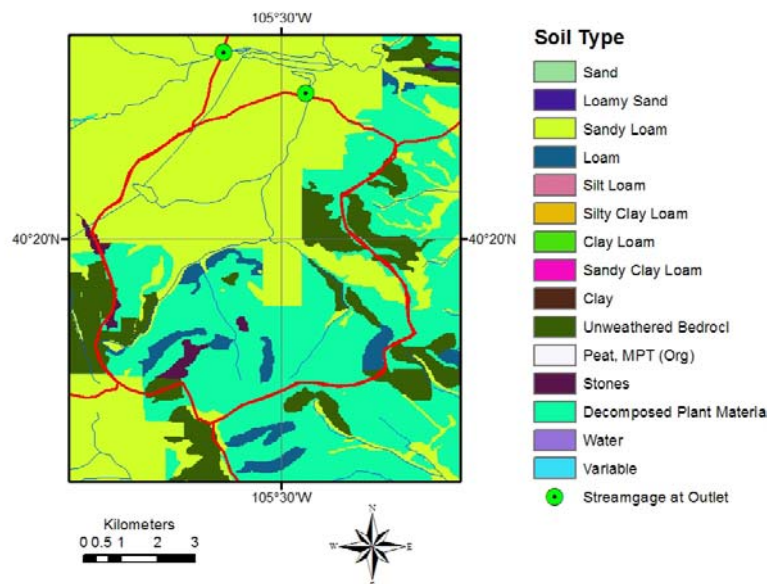

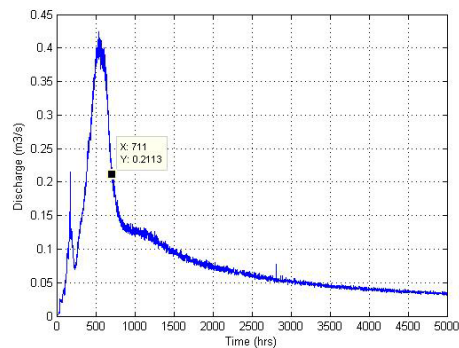**Figure 13. Soil distribution in Fish Creek watershed.**

Figure 14. Baseflow discharge from the drainage experiment for Fish creek basin.

4.2. Initial Groundwater Table

4.2.1 Drainage experiment

The initial groundwater table field can be imposed in a synthetic fashion through a groundwater rating curve relating the water table position to the basin baseflow. For this reason, a drainage experiment was conducted by setting the groundwater table at the land surface and allowing it to drain under the influence of gravity for a long period of time, without precipitation or evapotranspiration forcing. Streamflow generated by a drainage experiment is primarily dependent on the topography and soils characteristics. The resulting baseflow discharge is shown in Figure 13. Each drainage experiment has a typical hydrograph shape with rising and falling limbs which obey to the morphometric and soils properties of the basin. This spin-up exercise will allow extracting the groundwater initial table elevation for which the drained discharge (falling limb) equals the observed discharge (Q_{1st_July} = 0.23 m^3/s) at the beginning of the simulation. In our case, this discharge occurred after 711 hours of drainage. The groundwater table corresponding to this hour was selected as the initial condition to conduct a first simulation with the complete set of inputs between July 1st and July 30th, 2004.

4.2.2 Periodic forcing for initialization

Another initialization strategy explored to find a feasible initial groundwater table is based on setting up a periodic forcing. For this setup, the model is run for 5 consecutive July months with identical inputs. This process is sometimes called in the literature as reaching a dynamic equilibrium through periodic forcing. The final groundwater condition resulting from this dynamic equilibrium was used as the initial condition for the actual simulation. Results are illustrated in section 4.3.
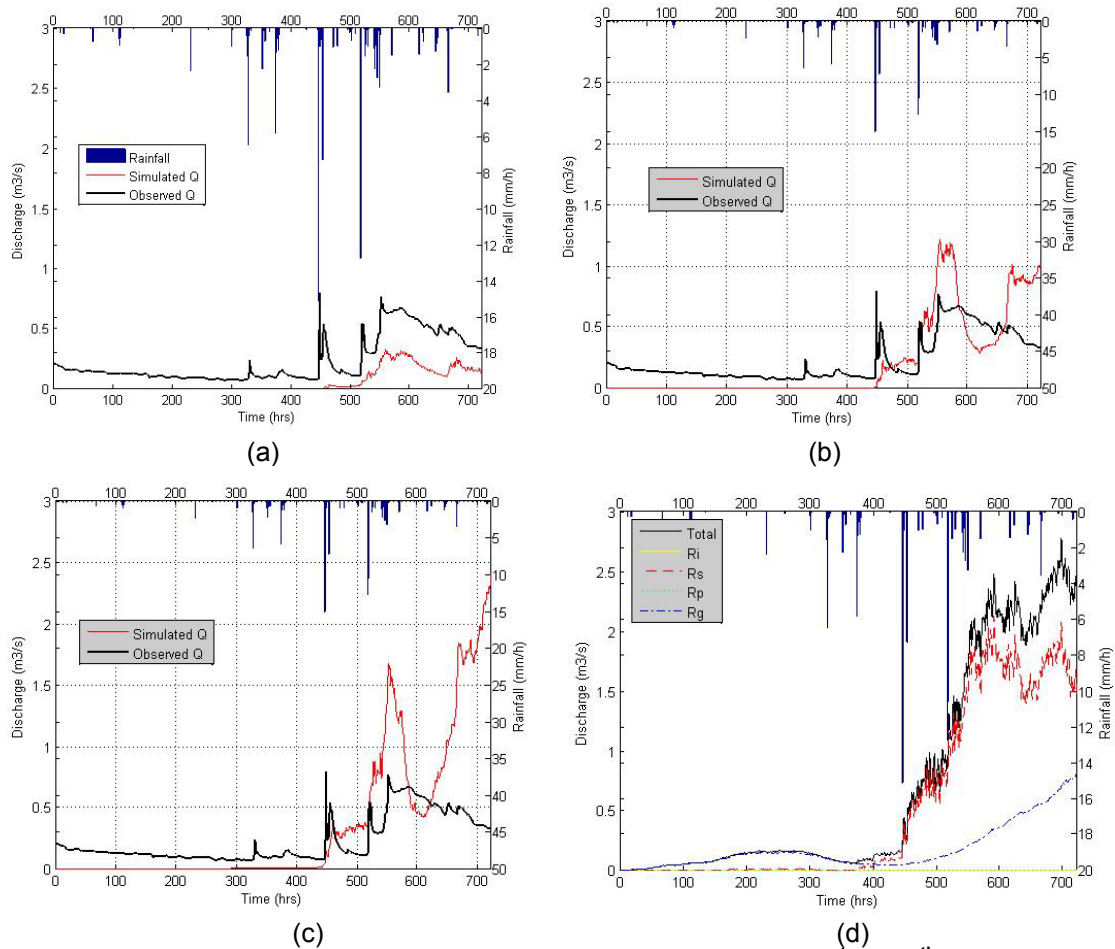
(a)

(b)

(c)

(d)

Figure 15. Preliminary streamflow simulation for the period July 1st to 30th, 2004 for three different groundwater table initial conditions: (a) Very dry state, (b) Drainage experiment, and (c) Periodic forcing .

4.3. Preliminary Simulation Results

Figure 14 illustrates the observed and simulated streamflows at the outlet of Fish Creek watershed for three conditions of the initial groundwater table: (a) Initial groundwater elevation field corresponding to drainage experiment up to very dry conditions, (b) Initial groundwater elevation field corresponding to the drainage experiment (for $Q_{Drain}=Q_{obsjul1}$) and (c) Groundwater initial elevation obtained from the periodic forcing.

Each initial condition produces different watershed response. The extreme (a) initial condition, underestimates discharges over the all period. However, it presents a good trend and similarity to the observed discharges hydrograph shape when rainfall events are present (after hour 500). The condition (b), with a wetter initial condition, also underestimates the low discharges up to the hour 470. Thereafter, simulated streamflows overestimate several peaks between hours 500 and 600 and then a successive underestimation and overestimation of the streamflows can be seen between hours 600 and 720. Analogously, initial conditions for the groundwater table from the periodic forcing, (c), produce a significant overestimation of streamflows after time 470 hrs. A more detailed view

17

to the basin integrated runoff mechanisms for case (c) is shown by Figure 14(d). This figure illustrates the dominance of saturation excess and groundwater contribution to the total runoff after the time 450hr. This provides an idea of the importance of the groundwater-runoff contribution on the total discharge. We continue to work on these simulations to both improve the initial condition and determine appropriate model parameters.

5. Conclusions and Future Work

Eleven sub-basins, belonging to Big Thompson, Saint Vrain, Boulder and Coal Creek, and their most relevant data sets, have been collected during this project period. These basins have been selected through a multiple step analysis based on available data and hydrological characteristics. They span a large range of contributing areas and are characterized by lacking major dams and other hydraulic structures, thus ensuring natural hydrologic response. Digital elevation models, basin boundaries, stream networks, soil and vegetation maps, and hydrometeorological observations have been collected to provide input and verification data for the hydrologic modeling efforts in the project.

Preliminary simulations were conducted with the aim of testing the model performance. Discharges at Fish Creek for the simulation period are sensitive to the groundwater table initial condition. Drainage experiment output as an initial condition underestimates discharge in the first half of the simulation, but overestimates several peaks between hours 500 and 600. Analogously, initial conditions for the groundwater initial table from the periodic forcing, amplifies the above mentioned effect when significant and consecutive precipitation events are present. A close view to the runoff mechanism illustrates the dominance of saturation excess runoff, directly linked to variable source area concept, and the groundwater contribution itself.

As next steps in the project development an evaluation of the available QPEs and QPFs will be performed. NEXRAD-MPE, NEXRAD level II and PERSIANN CCS will be evaluated in light of error sources due to their generation algorithms. Once this evaluation has been performed, model calibration for one basin, for several periods/events of interest, will be made. This next step includes: (a) Parameter uncertainty handling, by utilizing a range of parameter values from a feasible distribution, and (b) Initial condition uncertainty through the imposing of groundwater table elevation. These two steps will allow evaluation of the precipitation product type on the flood forecasting skill. Additionally, work will also proceed on developing an ensembling technique for the TITAN nowcasting system which will permit a probabilistic generation of short-term QPFs for use in flash flood modeling.

References

Brutasert, W. 2005. Hydrology - An Introduction. Cambridge Univ. Press, New York, NY; 605pp.

Dixon, M., 1994. Automated Storm Identification, Tracking and Forecasting – A radar-based methodology. Cooperative thesis No. 148. NCAR/CT-148, 180 pages.

Ivanov VY, Vivoni ER, Bras RL, Entekhabi D. 2004a. Catchment hydrologic response with fully distributed triangulated irregular network model. *Water Resources Research* 40: W11102.

Ivanov VY, Vivoni ER, Bras RL, Entekhabi D. 2004b. Preserving high-resolution surface and rainfall data in operational-scale basin hydrology; a fully-distributed physically-based approach. *Journal of Hydrology* 298: 80–111.

Kelsch, M. 1988. An evaluation of the NEXRAD hydrology sequence for different types of convective storms in Northeastern Colorado. Internal report to PROFS, NOAA-ERL, Boulder, CO.

Mahmood, T. and Vivoni, E. 2008. Evaluation of distributed soil moisture simulations through field observations during the North American monsoon in Redondo Creek, New Mexico. *Ecohydrology,* 1(3): 271-287.

Mascaro, G., Vivoni, E.R., Deidda, R. 2006. Evaluation of Uncertainty in Nested Flood Forecasts by Coupling a Multifractal Precipitation Downscaling Model and a Fully-Distributed Hydrological Model. *AGU Fall Conference*, San Francisco, CA.

Ogden, F. 1997. CASC2D Reference Manual. Dpt of Civil and Environmental Engineering, Univ of Connecticut. 77 pp.

Rawls WJ, Brakensiek DL, Miller N. 1983. Green-Ampt infiltration parameters from soil data. *Journal of Hydraulic Engineering* 109(1): 62–70.

Rutter, A. J., Kershaw. K. A., Robins, P.C. & Morton, A. J. 1971. A predictive model of rainfall interception in forests. I. Derivation of the model from observations in a plantation of Corsican pine. *Agric. Meteorol*. 9, 367-87.

Rutter, A. J., A.J. Morton, and Robins, P.C. 1975. A predictive model of rainfall interception in forests. II. Generalization of the model and comparison with observations in some coniferous and hardwood stands. *J. appl. Ecol*. 12, 367-80

Rutter, A. J., A.J. Morton, and Robins, P.C. 1977. A predictive model of rainfall interception in forests. III. Sensitivity of the model to stand parameters and meteorological variables. *J. appl. Ecol.* 14, 567-88

Wilks, D. S. 2005. Statistical Methods in the Atmospheric Sciences. 648pp.